Influence of a strong laser field on the Coulomb explosion and the stopping power of fast C_{60} clusters in plasmas

Gui-Qiu Wang,[1,*] Peng E,[2,†] Tao Ma,[1] You-Nian Wang,[3] Li Yao,[1] Yao-Chuan Wang,[1] Da-Jun Liu,[1] Hong Gao,[1] Zhang-Hu Hu,[3] Fang-Shuai Duan,[2] Hai-Yang Zhong,[1] Li-Hong Cheng,[1] Kun Yang,[1] Wei Liu,[1] Min Sun,[1] and Dian-Guo Xu[2]

[1]*Institute of Computational Physics, Department of Physics, Dalian Maritime University, Dalian 116026, China*

[2]*Department of Electrical Engineering, Harbin Institute of Technology, Harbin 150001, China*

[3]*Department of Physics, Dalian University of Technology, Dalian 116023, China*

(Received 10 August 2012; published 8 October 2012)

The influence of a high-intensity laser field on the Coulomb explosion and stopping power for a swift C_{60} cluster ion in a plasma target is studied by means of the molecular dynamics method based on the linearized Vlasov-Poisson theory. In the presence of the laser field, the general expressions for the induced potential in the target among the ions within the cluster are derived. Based on the numerical solution of the equations of motion for the constituent ions, the Coulomb explosion patterns and the cluster's stopping power are discussed for a range of laser and plasma parameters. Numerical results show that the laser field affects the correlation between the ions and contributes to weakening the wake effect and the stopping power as compared to the laser-free case. On the other hand, the vicinage effects in the cluster Coulomb explosion dynamics and the stopping power are strongly affected by the variations in the laser parameters, cluster speed, and plasma parameters. For example, Coulomb explosions are found to be hindered in the longitudinal expansion with the increasing of laser intensity and laser angle, and the Coulomb explosions proceed faster for lower plasma densities and higher electron temperatures.

DOI: 10.1103/PhysRevA.86.043201 PACS number(s): 36.40.−c, 34.50.Bw, 52.40.Mj, 79.20.Eb

I. INTRODUCTION

Recent developments in laser technology are already capable of producing ultrashort pulses with focal intensities up to 10^{21} W/cm^2 [1], which has given rise to the possibility of new studies of interaction processes for applications in optics, solid-state, and fusion research. In particular, a promising inertial confinement fusion scheme has been recently proposed [2,3], in which a plasma target is radiated simultaneously by both an intense laser beam and an intense ion beam. Within this scheme, several experiments [4–7] have been devoted to measuring the energy losses and charge states of heavy-ion beams in the laser-ablated plasma targets.

Understanding the interaction of energetic cluster ion beams with the plasma target in the presence of a laser field is of crucial importance due to their ability to deposit energy in a small region of the target [8,9]. Coulomb explosion and stopping power are two important quantities for this course. In theoretical aspects, Arista first developed a general formulation [10], based on a time-dependent Hamiltonian, to describe the effect of a strong laser field on the energy loss of a swift ion moving in a degenerate electron gas. For plasma targets, on the other hand, it was found that the effect of the laser field is to decrease the energy losses when the projectile velocity is smaller than the plasma electron thermal velocity [11], and projectile particles may be accelerated by the laser field in the high-intensity limit [12]. Silva and Galvão have studied the effects of the laser field on the energy loss of ion clusters moving in a hot plasma [13], and found that the laser field affected the spatial correlation among the cluster constituent particles and induced a decrease of the energy loss, when compared to a laser-free case. Recently, Nersisyan and Deutsch studied the stopping of ions in a plasma irradiated by an intense laser field and found that the radiation field might strongly reduce the mean energy loss for slow ions while increasing it at high velocities [14]. In addition, Hu *et al.* used a two-dimensional particle-in-cell simulation to investigate the dynamic polarization and stopping power for an ion beam propagating through a two-component plasma, which is simultaneously irradiated by a strong laser pulse [15]. However, Coulomb explosion effects of the cluster were not included in the work mentioned above.

In fact, Coulomb explosion is a very interesting phenomenon for fast clusters traveling in plasmas [16–18], especially for larger clusters such as C_{60}. When a fast cluster enters a target, it will be quickly stripped of its valence electrons, and further penetration of the resulting constituent ions will be accompanied by simultaneous processes of Coulomb explosion and the energy deposition into the electron excitations of the target. In the presence of a high-intensity laser field, the laser parameters will affect the Coulomb explosions and the energy losses. The relevant results have been discussed in a solid target [19]. As far as the C_{60} cluster is concerned, the penetration phenomena have been studied soon after Kroto's team first discovered C_{60} clusters in the laboratory in 1985 [20]. The Orsay group was the first to measure the energy losses of energetic C_{60} clusters in thin carbon foils [21]. Also, the track formation has been observed experimentally in metals, insulators, and semiconductors under the irradiation by fast C_{60} cluster beams [22–25]. On the theoretical side, Nardi and Zinamon [26] were the first to study the Coulomb explosion of fast C_{60} clusters in solids by means of molecular dynamics (MD) simulations [26]. Zwicknagel and Deutsch [27] studied the correlation effects in the stopping of C_{60} by using the random-phase approximation (RPA) dielectric function for a free-electron target, and they also treated the Coulomb explosion by means of a Yukawa-like inter-ionic

*gqwang@dlmu.edu.cn
†epeng@hit.edu.cn

potential. Wang and Qiu [28] considered the wake effects in the MD simulations of the C_{60} coulomb explosions in a solid Al target, and the dynamically screened inter-ionic potential was taken fully into account. The results showed that the explosion patterns of fast C_{60} clusters exhibited strong asymmetries after long penetration times and the corresponding comments have been given by Avalos *et al.* [29]. For a plasma target, we have studied Coulomb explosions and energy losses of C_{60} clusters, showing that the Coulomb explosion patterns of fast C_{60} clusters can be affected strongly by the projectile speed and plasma parameters [17]. However, it is worth mentioning that the influence of the laser field was not considered in these studies.

In this work, we present a study of the influence of a high-intensity laser field on Coulomb explosions and the stopping power of a C_{60} cluster in a plasma target based on the linearized Vlasov-Poisson theory. The aim is to study the influence of laser field on the Coulomb explosion and stopping power of the cluster and reveal the vicinage effect and the wake effect in the dynamic polarization of the plasma. The paper is organized as follows. In Sec. II, following the linearized Vlasov-Poisson equations, we use a Fourier-like analysis to derive general expressions for the laser-assisted dynamically screened interaction potential among the constituent ions in a correlated-ion cluster moving in a plasma target. We study the effects of the laser field on the Coulomb explosion dynamics of the correlated-ion cluster by solving the equations of motion for the constituent ions. In Sec. III, the modifications of the laser-assisted energy losses of the C_{60} cluster due to Coulomb explosion are discussed for prolonged penetration time. Finally, a brief summary of the results is presented in Sec. IV.

II. COULOMB EXPLOSIONS

Let us first consider an ion with the charge number Z_1 and the projectile velocity $\mathbf{v}$ moving through a plasma target with the density n_0 and the electron temperature T_e. Assuming that there are N electrons bound to the ion, its charge density is given by

$$\rho_{\rm ext}(\mathbf{r},t) = Z_1\, e\delta(\mathbf{r}-\mathbf{v}t) - e\rho_e(\mathbf{r}-\mathbf{v}t), \tag{1}$$

where $Z_1 e\delta(\mathbf{R})$ and $e\rho_e(\mathbf{R})$ ($\mathbf{R}=\mathbf{r}-\mathbf{v}t$) denote the nuclear and the bound electron charge densities, respectively, with $N=\int d\mathbf{R}\rho_e(\mathbf{R})$. We assume that the projectile velocity of the ion is far larger than the ion thermal velocity in the plasma, so we can only consider the contributions of the electron component of the plasma in the following discussion. Under the radiation of the laser field $\mathbf{E}_0(t)=\mathbf{E}_0\sin\omega_0 t$, the scalar potential $\Phi(\mathbf{r},t)$ yielded by the ion can be determined by the linearized Vlasov-Poisson equations

$$\left(\frac{\partial}{\partial t}+\mathbf{u}\cdot\frac{\partial}{\partial \mathbf{r}}\right) f_1(\mathbf{r},\mathbf{u},t) = \frac{e}{m_e}\left(\mathbf{E}_0\sin\omega_0 t - \frac{\partial\Phi}{\partial\mathbf{r}}\right)\cdot\frac{\partial f_0(\mathbf{u})}{\partial\mathbf{u}}, \tag{2}$$

$$\nabla^2\Phi(\mathbf{r},t) = 4\pi\left[e n_1(\mathbf{r},\mathbf{t}) - \rho_{\rm ext}(\mathbf{r},t)\right], \tag{3}$$

where f_1 is the perturbed electron distribution function, f_0 is the unperturbed electron distribution function which is taken to be a uniform Maxwellian distribution, and $n_1(\mathbf{r},\mathbf{t}) = \int d\mathbf{u} f_1(\mathbf{r},\mathbf{u},t)$ is the perturbed electron density. Similarly to the work of Brandt and Kitagawa (BK) [30], we choose the form of $\rho_e(\mathbf{R})$ as

$$\rho_e(\mathbf{R}) = N\exp(-R/\Lambda)/(4\pi R\Lambda^2), \tag{4}$$

where Λ is the screening length of the ion. Following the BK variational approach, D'Avanzo presented an extrapolating expression of the number of bound electrons per unit ion charge state $\eta = N/Z_1$ for a heavy ion in plasmas [31]

$$\eta = \frac{2}{9}\sqrt{\frac{2}{3\pi}}\frac{\sqrt{Z}}{[1+(v/v_T)^2]^{3/2}}, \tag{5}$$

in terms of the screening length

$$\Lambda/\lambda_D = \left(\frac{2\pi}{27}\right)^{1/4} Z^{1/4}, \tag{6}$$

where $Z = Z_1/N_D$; $N_D = n_0\lambda_D^3$ is the number of particles in a typical Debye volume. $\lambda_D = \sqrt{k_B T_e/4\pi e^2 n_0}$ is the electron Debye screening length.

By solving Eqs. (1) and (2) in the space-time Fourier-like transform

$$A(\mathbf{r},t) = \int\int \frac{d\mathbf{k}d\omega}{(2\pi)^4} A(\mathbf{k},\omega)e^{i\mathbf{k}\cdot\mathbf{s}-i\omega t}, \tag{7}$$

where $A(\mathbf{r},t)$ stands for any of the perturbed quantities in the shifted frame of reference, $\mathbf{s}=\mathbf{r}-\mathbf{a}_E\sin(\omega_0 t)$. With this transform, the scalar potential is readily obtained as follows:

$$\Phi(\mathbf{k},\omega) = \frac{4\pi\rho_{\rm ext}(\mathbf{k},\omega)}{k^2\varepsilon(k,\omega)}, \tag{8}$$

where $\varepsilon(k,\omega)$ is the longitudinal dielectric function of the classical electron plasma

$$\varepsilon(k,\omega) = 1 + (k\lambda_D)^{-2}[X(\omega/kv_T) + iY(\omega/kv_T)], \tag{9}$$

with $X(\varsigma) = 1 - 2\varsigma e^{-\varsigma^2}\int_0^\varsigma e^{t^2}dt$ and $Y(\varsigma)=\sqrt{\pi}\varsigma e^{-\varsigma^2}$. Here $v_T=\sqrt{k_B T_e/m_e}$ is the electron thermal speed. In Eq. (8), $\rho_{\rm ext}(\mathbf{k},\omega) = Z_1 e\int dt\exp[-i\mathbf{k}\cdot\mathbf{a}_E\sin(\omega_0 t) + i(\omega - \mathbf{k}\cdot\mathbf{v})t]$ is the Fourier transform of the external charge density $\rho_{\rm ext}(\mathbf{r},t)$ and $\mathbf{a}_E = \mathbf{e}\mathbf{E}_0/(m_e\omega_0^2)$ is the transverse oscillation amplitude of electrons driven by the laser field (the so-called quiver amplitude). On using the Jacobi identity, $\exp[-i\mathbf{k}\cdot\mathbf{a}_E\sin(\omega_0 t)] = \sum J_n(\mathbf{k}\cdot\mathbf{a}_E)\exp(i\omega_0 t)$, we obtain

$$\rho_{\rm ext}(\mathbf{k},\omega) = 2\pi\rho_\eta(k)\sum_{n=-\infty}^{\infty} J_n(\mathbf{k}\cdot\mathbf{a}_E)\delta(\omega+n\omega_0-\mathbf{k}\cdot\mathbf{v}), \tag{10}$$

$$\rho_\eta(k) = Z_1 e\left(1-\frac{\eta}{1+(k\Lambda)^2}\right), \tag{11}$$

where $J_n(x)$ is the nth-order Bessel function of the first kind. With Eqs. (8) and (10), the scalar potential can be written as

$$\Phi(\mathbf{r},t) = \frac{1}{2\pi^2}\sum_{n,m}\int \frac{d^3k}{k^2}\rho_\eta(k)J_n(\mathbf{k}\cdot\mathbf{a}_E)J_n(\mathbf{k}\cdot\mathbf{a}_0) \times \frac{e^{i\mathbf{k}\cdot(\mathbf{r}-\mathbf{v}t)}e^{i(n-m)\omega_0 t}}{\varepsilon(k,\omega_n)}, \tag{12}$$

where $\omega_n = \mathbf{k}\cdot\mathbf{v} - n\omega_0$ is the laser-harmonic Doppler-shifted frequency.

Next consider a fast C_{60} cluster moving in the plasma. The interaction potential between the two constituent ions, located at $\mathbf{r}_j$ and $\mathbf{r}_l$, is expressed as

$$\begin{aligned} U(\mathbf{r},t) &= \int d\mathbf{r}'\rho_{\text{ext}}(\mathbf{r}'-\mathbf{r}_j,t)\Phi(\mathbf{r}'-\mathbf{r}_l,t) \\ &= \frac{1}{2\pi^2}\sum_{n,m}\int \frac{d^3k}{k^2}\rho_\eta^2(k)J_m(\mathbf{k}\cdot\mathbf{a}_0)J_n(\mathbf{k}\cdot\mathbf{a}_E) \\ &\quad\times \frac{e^{i\mathbf{k}\cdot(\mathbf{r}-\mathbf{v}t)}e^{i(n-m)\omega_0 t}}{\varepsilon(k,\omega_n)}, \end{aligned} \tag{13}$$

where $\mathbf{r}_{jl} = \mathbf{r}_j - \mathbf{r}_l$ is the relative position of the two ions and $\mathbf{v}$ is the velocity of the center of mass (CM) of the ion cluster. After taking the time average over the laser period in this expression, the fast oscillations with time t are moved by setting the factor $e^{i(n-m)\omega_0 t}$ to zero unless $m = n$. As a result, the average interaction potential becomes time independent; viz.,

$$U(\mathbf{r}_{jl}) = \frac{1}{2\pi^2}\sum_{n=-\infty}^{\infty}\int \frac{d^3k}{k^2}\rho_\eta^2(k)J_n^2(\mathbf{k}\cdot\mathbf{a}_E)\frac{e^{i\mathbf{k}\cdot\mathbf{r}_{jl}}}{\varepsilon(k,\omega_n)}. \tag{14}$$

In order to simplify the following calculations, we assume that the three vectors $\mathbf{E}_0$, $\mathbf{v}$, and $\mathbf{k}$ are all in the same plane and take α to be the angle between $\mathbf{E}_0$ and $\mathbf{v}$. On introducing the variable $\omega = \mathbf{k}\cdot\mathbf{v} = kv\cos\theta$, we define the quality

$$\chi(k,\omega) = \mathbf{k}\cdot\mathbf{a}_E = \frac{a_E\omega}{v}\cos\alpha - \kappa a_E\sin\alpha, \tag{15}$$

where $\kappa = \sqrt{k^2 - \omega^2/v^2}$. Assuming that the projectile velocity is directed along the z axis, the potential can be written in the cylindrical coordinates $\mathbf{r}_{jl} = (\rho_{jl}, z_{jl})$ as follows:

$$\begin{aligned} U(\rho_{jl},z_{jl}) &= \frac{2}{\pi v}\sum_{n=-\infty}^{\infty} \\ &\quad\times\int_0^{k_{\max}}\frac{dk}{k}\int_0^{kv} d\omega\rho_\eta^2(k)J_0(\rho_{jl}\kappa)J_n^2[\chi(k,\omega)] \\ &\quad\times\left\{\cos\left(\frac{\omega z_{jl}}{v}\right)\text{Re}\left[\frac{1}{\varepsilon(k,\omega)}\right]\right. \\ &\quad\left. -\sin\left(\frac{\omega z_{jl}}{v}\right)\text{Im}\left[\frac{1}{\varepsilon(k,\omega)}\right]\right\}, \end{aligned} \tag{16}$$

where $r_{jl} = \sqrt{\rho_{jl}^2 + z_{jl}^2}$. In Eq. (16) we have induced a cutoff wave number $k_{\max} = m_e(v^2 + 2v_T^2)/(Z_1 e)^2$ to avoid the divergence of the integral caused by incorrect treatment of the short-range interactions between the projectile and electrons in the plasma [32]. Actually, the integral is fast convergent as increasing the values of the upper limit $k_{\max}$ if the internuclear distance r keeps a limited value.

In the following discussions, we assume that the vacuum wavelength λ_0 of the laser field is larger than the Debye screening length λ_D and the electron oscillation amplitude a_E. Thus, the laser field should satisfy the constraints

$$\frac{\omega_0}{\omega_p} < \frac{2\pi c}{v_T} \tag{17}$$

and

$$I < \frac{1}{2}n_0 c(m_e c^2)\left(\frac{\omega_0}{\omega_p}\right)^2, \tag{18}$$

where $I = cE_0^2/8\pi$ is the intensity of the laser field and $\omega_p = \sqrt{4\pi n_0 e^2/m_e}$ is the plasma frequency. The above conditions can also used to estimate the plasma critical density n_c when the intensity and frequency of the laser field are given. For example, we get that the critical density is about $n_c = 10^{18}\ \text{cm}^{-3}$ for given $I = 1.2\times10^{15}\ \text{W/cm}^{-2}$ and $\omega_0 = \omega_p$.

Invoking the assumption of the adiabatic change of the inter-ionic distances during the propagation through the target, we can write the equation of motion for the position of the jth ion in the cluster CM frame of reference as follows:

$$m\frac{d^2\mathbf{r}_j}{dt^2} = \mathbf{F}_j^s(\mathbf{v}) + \sum_{j\neq l=1}^{60}\mathbf{F}(\mathbf{r}_{jl},\mathbf{v}), \tag{19}$$

where $\mathbf{r}_{jl} = \mathbf{r}_j - \mathbf{r}_l$ is the position vector of the jth ion relative to the lth ion. The self-stopping forces and the interaction forces are obtained from the inter-ionic interaction potential $U(\mathbf{r}_{jl},\mathbf{v})$, respectively, as follows:

$$\mathbf{F}_j^s(\mathbf{v}) = -\partial U(\mathbf{r}_{jl},\mathbf{v})/\partial\mathbf{r}_{jl}|_{\mathbf{r}_{jl}=0}, \tag{20}$$

$$\mathbf{F}(\mathbf{r}_{jl},\mathbf{v}) = -\partial U(\mathbf{r}_{jl},\mathbf{v})/\partial\mathbf{r}_{jl}, \quad j\neq l. \tag{21}$$

Under the assumptions that all ion charges are the same throughout the cluster and are constant during the Coulomb explosion, it is obvious that the self-stopping forces do not influence the evolution of the cluster structure. The equations of motion (19) are solved numerically for all ions in the cluster ($j = 1,2,\ldots,60$) subject to the set of the initial conditions $\mathbf{r}_j(0) = \mathbf{r}_{j0}$ characterizing the equilibrium structure of C_{60}, and with all the initial velocities in the CM frame being set to zero, $\dot{\mathbf{r}}_j(0) = 0$, based on the neglect of thermal vibrations of the constituent atoms.

Figure 1 shows several snapshots of the ion positions in the cluster CM frame at the penetration times $t = 0,5,10,15,20$, and 25 fs for a C_{60} cluster entering a plasma target with $T_e = 2$ eV and $n_0 = 10^{16}\ \text{cm}^{-3}$ at the speed $v = 3v_T$ for (a) no laser and (b) $a_E = 2\lambda_D$ and $\alpha = \pi/3$. It is interesting that the C_{60} cluster structure evolves into a basket-like shape, which becomes increasingly elongated in the direction of motion with the increasing time as a direct consequence of the wake-potential asymmetry in the inter-ionic forces. By comparison, one can see that the laser field weakened the wake effect contrast to the laser-free case. In order to further show the influence of laser intensity for Coulomb explosion, we plot Fig. 2. Figure 2 shows the influence of different laser intensities

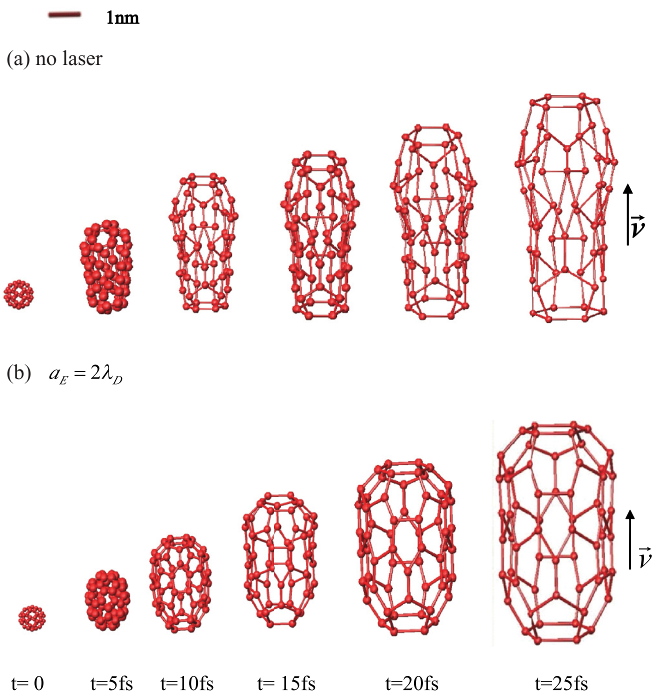

FIG. 1. (Color online) 3D Coulomb explosion patterns obtained for C_{60} moving at the speed $v = 3v_T$ in the indicated direction through a plasma target with the density $n_0 = 10^{16}$ cm^{-3} and the electron temperature $T = 2$ eV for (a) no laser and (b) $a_E = 2\lambda_D$ and $\alpha = \pi/3$. Snapshots of ion positions are given in a moving frame of reference attached to the cluster, for several penetration times: $t = 0,5,10,15,20,$ and 25 fs.

$a_E = \lambda_D, 2\lambda_D, 3\lambda_D, 4\lambda_D$ on the Coulomb explosion patterns after 25 fs for a C_{60} cluster entering a plasma target with $\alpha = \pi/3$ and other parameters are set as same as those used in Fig. 1. The results show that the Coulomb explosion proceeds slower in the longitudinal expansion along with the strengthen of laser intensity. At the same time, the C_{60} cluster asymmetric structure becomes not obvious, which indicates that the wake effect is weakened for higher laser intensity. Figure 3 shows the influences of different laser angles $\alpha = 0,\pi/6,\pi/3,\pi/2$ on the Coulomb explosion after 25 fs for C_{60} cluster entering a plasma

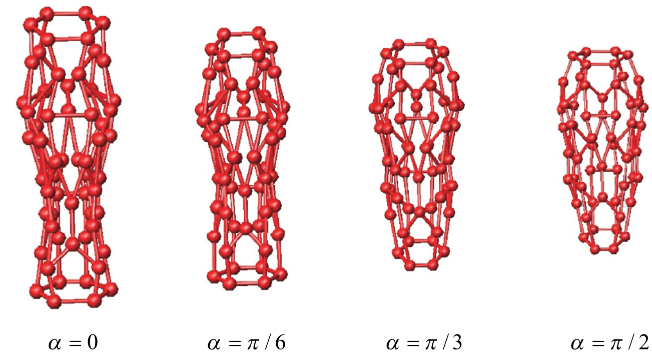

FIG. 3. (Color online) The influence of various laser angles $\alpha = 0,\pi/6,\pi/3,\pi/2$ on the Coulomb explosion after 25 fs for a C_{60} cluster entering a plasma target with $a_E = 2\lambda_D$ and other parameters are set as same as those used in Fig. 1.

target with $a_E = 2\lambda_D$ and other parameters are set as same as those used in Fig. 1. It can be seen that the results are very similar to Fig. 2. In general, the Coulomb explosion proceeds slower in the longitudinal direction as the angle increases from 0 to $\pi/2$, and the wake effect becomes weak to the increasing angle.

Figure 4 shows the influence of the plasma density $n_0 = 10^{16}$ cm^{-3}, 5×10^{16} cm^{-3}, 10^{17} cm^{-3} on the patterns of Coulomb explosion after 25 fs for a C_{60} cluster entering a plasma target with $T_e = 5$ eV, $v = 3v_T$, $a_E = 2\lambda_D$, and $\alpha = \pi/3$. Interestingly, the longitudinal expansion of the cluster remains insensitive to the changes in density, whereas the transversal size of the cluster grows faster as the density decreases. Figure 5 shows the effects of changing plasma temperature $T_e = 1$ eV, 5 eV, 10 eV on the Coulomb explosion patterns after 25 fs with $n_0 = 10^{16}$ cm^{-3} and other parameters are set the same as in Fig. 4. It is seen that as the temperature decreases, the longitudinal expansion of the cluster is promoted, whereas the transversal expansion is hindered. From Figs. 4 and 5 it follows that in classical high-temperature and low-density plasmas, the Coulomb explosion patterns are very close to the spherically symmetric or isotropic expansion picture of C_{60}. On the other hand, in the limit of cold and dense plasmas, corresponding to the degenerate electron gas

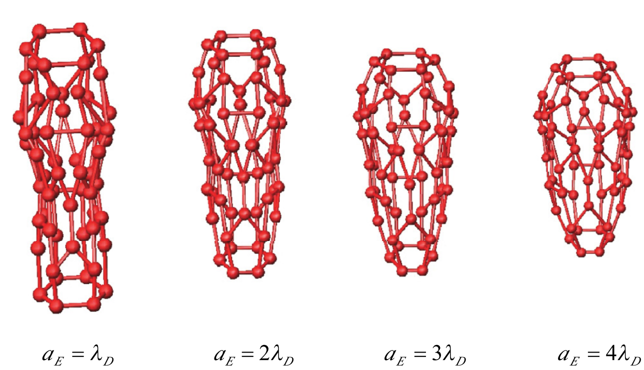

FIG. 2. (Color online) The influence of various laser intensities $a_E = \lambda_D, 2\lambda_D, 3\lambda_D, 4\lambda_D$ on the Coulomb explosion patterns after 25 fs for a C_{60} cluster entering a plasma target with $\alpha = \pi/3$ and other parameters are set as same as those used in Fig. 1.

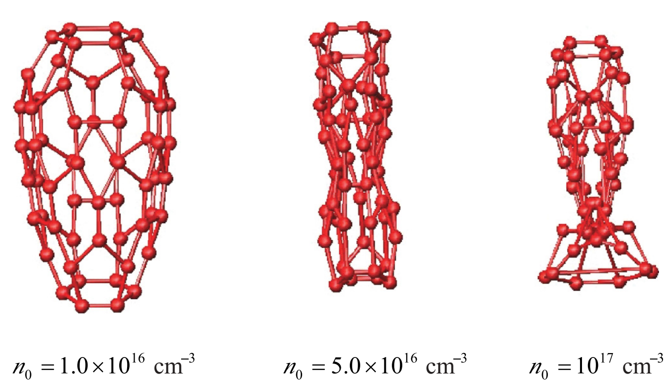

FIG. 4. (Color online) The influence of various plasma densities, $n_0 = 10^{16}$ cm^{-3}, 5×10^{16} cm^{-3}, 10^{17} cm^{-3} on the Coulomb explosion patterns after 25 fs for a C_{60} cluster entering a plasma target with $T_e = 5$ eV, $v = 3v_T$, $a_E = 2\lambda_D$, and $\alpha = \pi/3$.

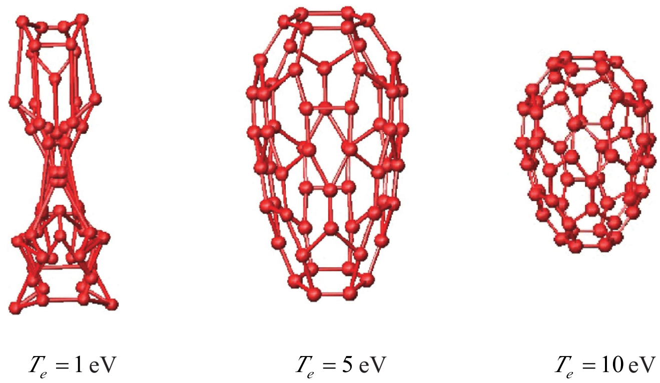

FIG. 5. (Color online) The influence of various electron temperatures $T_e = 1$ eV, 5 eV, 10 eV on the Coulomb explosion patterns after 25 fs with $n_0 = 10^{16}$ cm^{-3} and other parameters are set same as Fig. 4.

in solid targets, the explosion patterns are very much narrower and elongated in the direction of cluster motion.

III. STOPPING POWER

In the simulation, one can obtain the expression for the total cluster stopping power, assuming that the cluster moves in the z direction, as follows:

$$S_{cl}(v,t) = S_0(v) + S_v(v,t), \tag{22}$$

where $S_0(v) = -\sum_{j=1}^{60} F_s(v)$ is the contribution from the individual self-stopping forces, while $S_v(v,t) = -\sum_{j=1}^{60} \sum_{j\neq l=1}^{60} (\mathbf{F}_{jl})_z(\mathbf{r}_{jl},\mathbf{v})$ is the vicinage stopping power which describes interferences in the energy losses due to the spatial correlation among the constituent ions.

Figures 6(a) and 6(b) show the effect of laser parameters on self-stopping S_0 for a C_{60} cluster entering a plasma target with $T_e = 2$ eV and $n_0 = 10^{16}$ cm^{-3} at the speed $v = 3v_T$ for various (a) laser densities $a_E = 0,2\lambda_D,5\lambda_D$ and (b) laser angles $\alpha = \pi/6,\pi/3,\pi/2$. It is shown that the self-stopping S_0 increases with enhancement of penetration time, and this enhancement is faster in the early stages of penetration due to larger speed at the initial stages. Figures 7(a)–7(e) show that the total cluster stopping power S_{cl} varies with the penetration time for various (a) laser intensities $a_E = 0,2\lambda_D,5\lambda_D$, (b) laser angles $\alpha = \pi/6,\pi/3,\pi/2$, (c) projectile speeds $v = v_T,2v_T,3v_T$, (d) plasma densities $n_0 = 0.5 \times 10^{16}$ cm^{-3}, 1.0×10^{16} cm^{-3}, 2.5×10^{16} cm^{-3}, and (e) electron temperatures $T = 2$ eV, 10 eV, 100 eV. In general, the total cluster stopping power S_{cl} decreases with enhancement of penetration time. It is shown that the contribution of vicinage stopping to the total cluster stopping power is the main one. In addition, the initial value of the stopping power is greater for lower laser intensities, smaller laser angles, greater projectile speeds, lower plasma densities, and higher electron temperatures.

In order to further clarify the role of Coulomb explosion in diminishing the vicinage effect on the cluster energy loss, we show in Figs. 8(a)–8(e) the stopping power ratio, $R = 1 + S_v(v,t)/S_0(v)$, as a function of the penetration time t. Figures 8(a)–8(e) show that the stopping power ratio R decreases with enhancement of penetration time. One can also see that in the very early stages of Coulomb explosions, the stopping ratio reaches quite high values, indicating that constructive interferences in the vicinage effect can drastically increase the energy losses when the constituent ions are still close to each other. In particular, this enhancement of the energy loss is greater for lower laser intensities, smaller laser angles, faster projectiles, lower plasma densities, and higher electron temperatures. On the other hand, for prolonged penetration times t, the stopping ratio R approaches 1, indicating that the constituent ions of the cluster have moved so far away from each other in the course of Coulomb explosion that they essentially behave as independent projectiles.

IV. SUMMARY

We used the MD simulation method to study the influence of a strong laser field on the Coulomb explosion dynamics and the vicinage effects on the stopping power of swift C_{60} clusters in the classical plasma targets based on the linearized Vlasov-Poisson theory. In particular, we have focused on the laser-field effects and plasma parameters on the dynamically screened inter-ionic interaction governing the Coulomb explosion of the cluster which, in turn, is responsible for weakening of vicinage

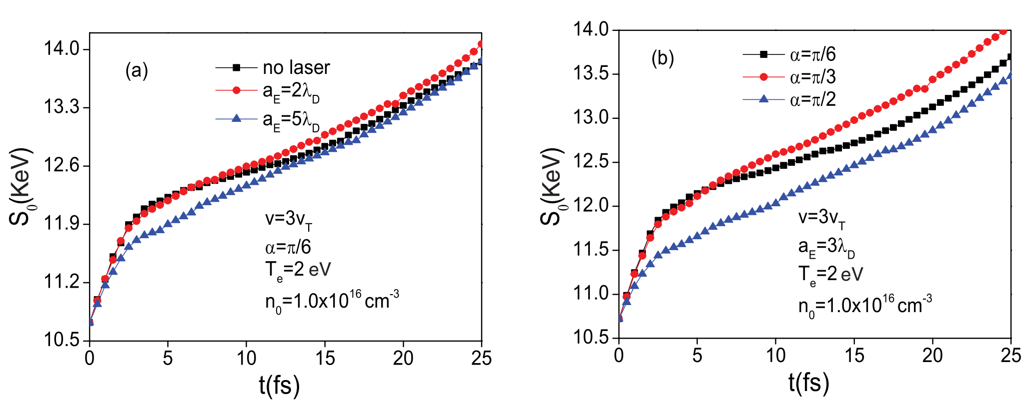

FIG. 6. (Color online) The self-stopping S_0 as a function of the penetration time t for a C_{60} cluster moving through a plasma target with $T_e = 2$ eV and $n_0 = 10^{16}$ cm^{-3} at the speed $v = 3v_T$ for various (a) laser densities $a_E = 0,2\lambda_D,5\lambda_D$ and (b) laser angles $\alpha = \pi/6,\pi/3,\pi/2$, and other parameters as shown in the figures.

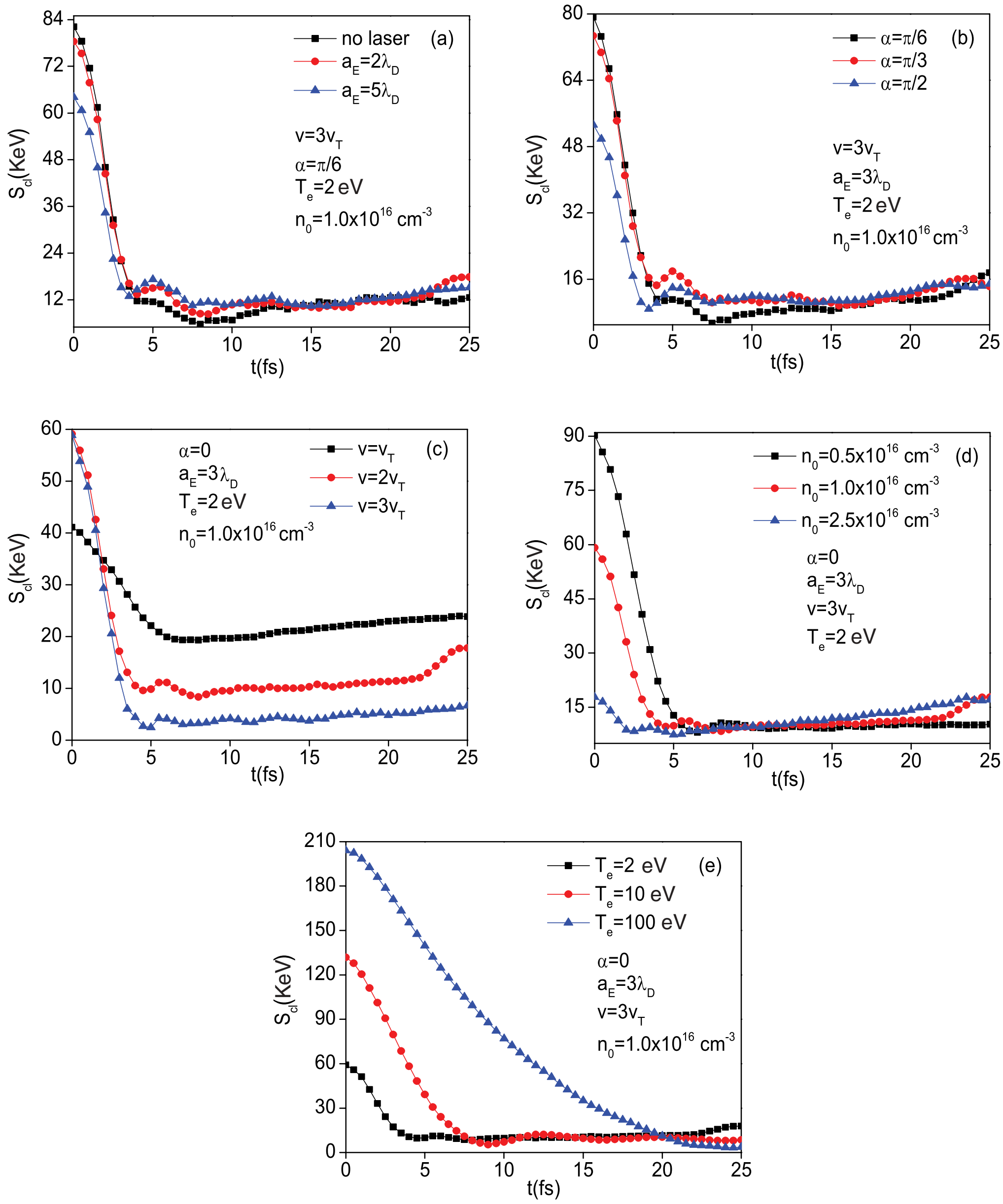

FIG. 7. (Color online) The influence of various (a) laser intensities $a_E = 0,2\lambda_D,5\lambda_D$, (b) laser angles $\alpha = \pi/6,\pi/3,\pi/2$, (c) projectile speeds $v = v_T,2v_T,3v_T$, (d) plasma densities $n_0 = 0.5 \times 10^{16}$ cm^{-3}, 1.0×10^{16} cm^{-3}, 2.5×10^{16} cm^{-3}, and (e) electron temperatures $T = 2$ eV, 10 eV, 100 eV on the total cluster stopping power as a function of the penetration time t for Coulomb explosion of C_{60} moving through a plasma target, and other parameters as shown in the figures.

effects on the energy loss of the cluster with increasing dwell time through the target.

Using the classical plasma dielectric function, the laser-assisted expressions for the interaction potential among the ions have been derived by means of a Fourier-like transform. By solving the equations of motion for individual ions numerically, the Coulomb explosion patterns of fast C_{60} clusters were revealed. In particular, it was found that the C_{60} cage structure becomes increasingly elongated in the direction of cluster motion, for a range of cluster speeds, when the plasma density increases and its temperature decreases. In the opposite limit of hot and low-density plasmas, the shape of C_{60} tends to retain a spherical symmetry in the course of Coulomb explosion. On the other hand, the Coulomb explosion proceeds slower in the longitudinal expansion along with the strengthening of laser intensity and angle. At the same time, the C_{60} cluster asymmetric structure becomes not obvious, which indicates the wake effect is weakened for higher laser intensity and angle.

Regarding the vicinage effects on the cluster energy losses, the simulation results show a significant increase in the stopping power, in comparison with the case of independent ions, at the early stages of Coulomb explosion, when the constituent ions are still quite close to each other. In particular, this enhancement of the energy loss is greater for lower laser intensities, smaller laser angles, faster projectiles,

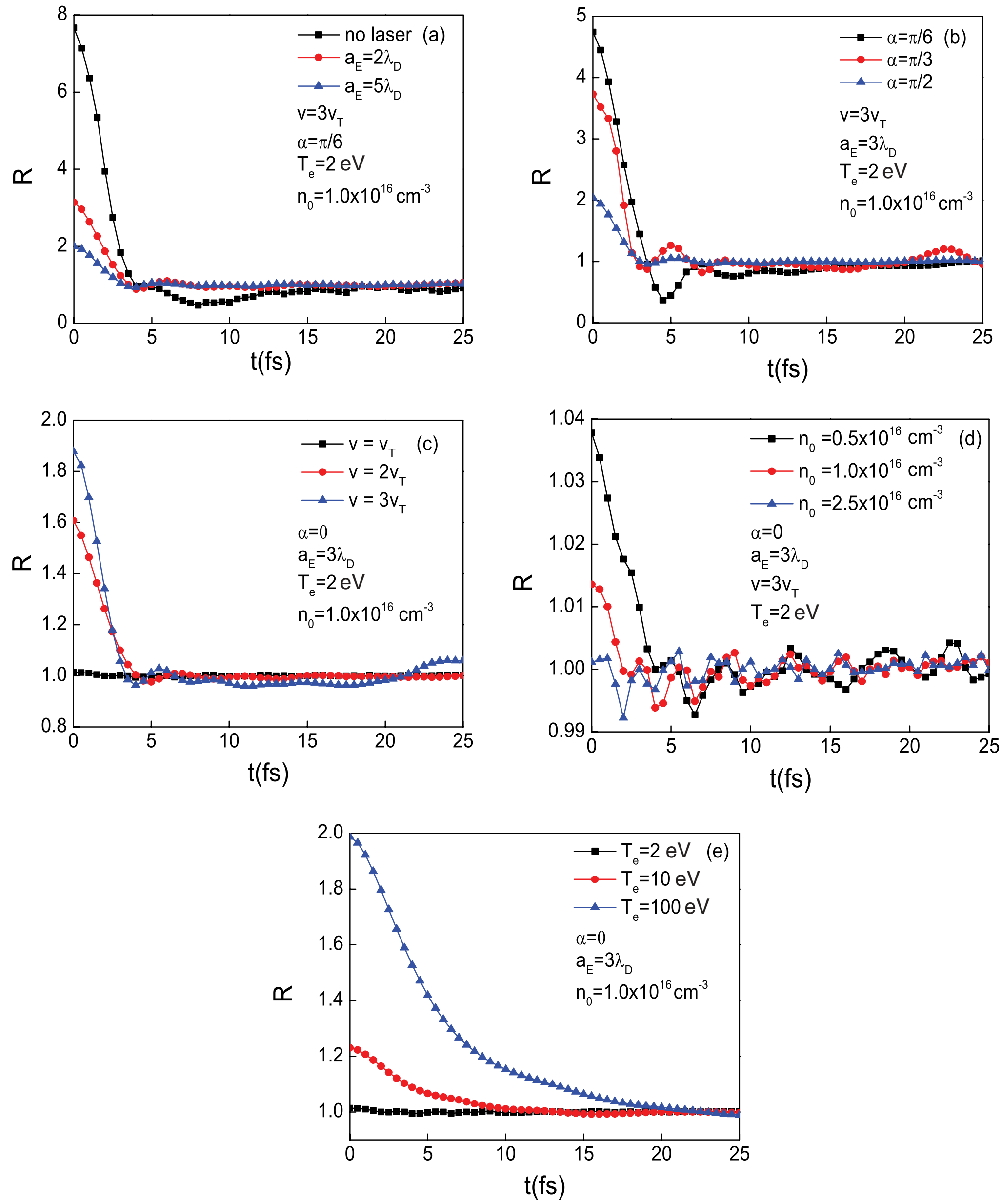

FIG. 8. (Color online) The influence of various (a) laser intensities $a_E = 0, 2\lambda_D, 5\lambda_D$, (b) laser angles $\alpha = \pi/6, \pi/3, \pi/2$, (c) projectile speeds $v = v_T, 2v_T, 3v_T$, (d) plasma densities $n_0 = 0.5 \times 10^{16}$ cm^{-3}, 1.0×10^{16} cm^{-3}, 2.5×10^{16} cm^{-3}, and (e) electron temperatures $T = 2$ eV, 10 eV, 100 eV on the stopping power ratio R as a function of the penetration time t for Coulomb explosion of C_{60} moving through a plasma target, and other parameters as shown in the figures.

lower plasma densities, and higher electron temperatures. For prolonged penetration times, the stopping power ratio falls faster, showing that the cluster longitudinal elongation due to the wake effects plays a significant role in diminishing the vicinage effect on cluster energy losses. Such conclusions may prove useful in future designs for the use of cluster ion beam to drive inertial confinement fusion.

ACKNOWLEDGMENTS

This work is jointly supported by the National Natural Science Foundation of China (Grants No. 10705007, No. 11005025, and No. 11105022), the National Basic Research Program of China (Grants No. 2010CB832901 and No. 2008CB717801), the Fundamental Research Funds for the Central Universities (Grants No. 2012TD018 and No. DUT10ZD111), the Program for New Century Excellent Talents in Universities (Grant No. NCET-08-0073), the Doctorial Start-Up Foundation of Liaoning Province in China (Grant No. 20071067), the Natural Science Foundation of Liaoning Province in China (Grants No. L2010055, No. L2010057, and No. 201102016), and the Natural Scientific Research Innovation Foundation at Harbin Institute of Technology (Grant No. 2009044).

[1] S. P. Hatchett, C. G. Brown, T. E. Cowan, E. A. Henry, J. S. Johnson, M. H. Key, J. A. Koch, A. B. Langdon, B. F. Lasinski, R. W. Lee, A. J. Mackinnon, D. M. Pennington, M. D. Perry, T. W. Phillips, M. Roth, T. C. Sangster, M. S. Singh, R. A. Snavely, M. A. Stoyer, S. C. Wilks, and K. Yasuike, Phys. Plasmas **7**, 2076 (2000).

[2] C. Stöckl, O. Boine-Frankenheim, and M. Roth, Laser Part. Beams **14**, 561 (1996).

[3] M. Roth, T. E. Cowan, M. H. Key, S. P. Hatchett, C. Brown, W. Fountain, J. Johnson, D. M. Pennington, R. A. Snavely, S. C. Wilks, K. Yasuike, H. Ruhl, F. Pegoraro, S. V. Bulanov, E. M. Campbell, M. D. Perry, and H. Powell, Phys. Rev. Lett. **86**, 436 (2001).

[4] K. Shibata, A. Sakumi, R. Sato, K. Tsubuku, J. Hasegawa, M. Ogawa, and Y. Oguri, Nucl. Instrum. Methods Phys. Res., Sect. B **161**, 106 (2000); **163**, 106 (2000).

[5] Y. Oguri, K. Tsubuku, A. Sakumi, K. Shibata, R. Sato, K. Nishigori, J. Hasegawa, and M. Ogawa, Nucl. Instrum. Methods Phys. Res., Sect. B **161–163**, 155 (2000).

[6] A. Frank, A. Blažević, P. L. Grande, K. Harres, T. Heßling, D. H. H. Hoffmann, R. Knobloch-Maas, P. G. Kuznetsov, F. Nürnberg, A. Pelka, G. Schaumann, G. Schiwietz, A. Schökel, M. Schollmeier, D. Schumacher, J. Schütrumpf, V. V. Vatulin, O. A. Vinokurov, and M. Roth, Phys. Rev. E **81**, 026401 (2010).

[7] D. H. H. Hoffmann, N. A. Tahir, S. Udreal, O. Rosmej, C. V. Meister, D. Varentsov, M. Roth, G. Schaumann, A. Frank, A. Blažević, J. Ling, A. Hug, J. Menzel, Th. Hessling, K. Harres, M. Günther, S. El-moussatil, D. Schumacher, and M. Imran, Contrib. Plasma Phys. **50**, 7 (2010).

[8] N. A. Tahir, K. J. Lutz, O. Geb, J. A. Maruhn, C. Deutsch, and D. H. H. Hoffmann, Phys. Plasmas **4**, 796 (1997).

[9] G. Zwicknagel and C. Deutsch, Phys. Rev. E **56**, 970 (1997).

[10] N. R. Arista, R. O. M. Galvão, and L. C. M. Miranda, Phys. Rev. A **40**, 3808 (1989).

[11] N. R. Arista, R. O. M. Galvão, and L. C. M. Miranda, J. Phys. Soc. Jpn. **59**, 544 (1990).

[12] H. B. Nersisyan and E. A. Akopyan, Phys. Lett. A **258**, 323 (1999).

[13] C. A. B. Silva and R. M. O. Galvão, Phys. Rev. E **60**, 7441 (1999).

[14] H. B. Nersisyan and C. Deutsch, Laser Part. Beams **29**, 389 (2011).

[15] Z. H. Hu, Y. H. Song, Z. L. Mišković, and Y. N. Wang, Laser Part. Beams **29**, 299 (2011).

[16] G. Q. Wang, Y. N. Wang, and Z. L. Mišković, Phys. Rev. E **68**, 036405 (2003).

[17] G. Q. Wang, Y. N. Wang, and Z. L. Mišković, Phys. Plasmas **12**, 042702 (2005).

[18] G. Q. Wang, W. K. Li, and Y. N. Wang, Chin. Phys. Lett. **26**, 125203 (2009).

[19] G. Q. Wang, Y. H. Song, Y. N. Wang, and Z. L. Mišković, Phys. Rev. A **66**, 042901 (2002).

[20] H. W. Kroto, J. R. Heath, S. C. O'Brien, and R. F. Curl, Nature (London) **318**, 162 (1985).

[21] K. Baudin, A. Brunelle, M. Chabot, S. Della-Negra, J. Depauw, D. Gardès, P. Håkansson, Y. Le Beyec, A. Billebaud, M. Fallavier, J. Remillieux, J. C. Poizat, and J. P. Thomas, Nucl. Instrum. Methods Phys. Res., Sect. B **96**, 341 (1994).

[22] H. Dammak, A. Dunlop, D. Lesueur, A. Brunelle, S. Della-Negra, and Y. Le Beyec, Phys. Rev. Lett. **74**, 1135 (1995).

[23] A. Dunlop, G. Jaskierowicz, J. Jensen, and S. Della-Negra, Nucl. Instrum. Methods Phys. Res., Sect. B **132**, 93 (1997).

[24] J. Jensen, A. Dunlop, S. Della-Negra, and H. Pascard, Nucl. Instrum. Methods Phys. Res., Sect. B **135**, 295 (1998).

[25] S. M. M. Ramos, N. Bonardi, B. Canut, S. Bouffard, and S. Della-Negra, Nucl. Instrum. Methods Phys. Res., Sect. B **143**, 319 (1998).

[26] E. Nardi and Z. Zinamon, Phys. Rev. A **51**, R3407 (1995).

[27] G. Zwicknagel and C. Deutsch, Nucl. Instrum. Methods Phys. Res., Sect. A **415**, 599 (1998).

[28] Y.-N. Wang, H.-T. Qiu, and Z. L. Mišković, Phys. Rev. Lett. **85**, 1448 (2000).

[29] S. Heredia-Avalos, C. D. Denton, R. Garcia-Molina, and I. Abril, Phys. Rev. Lett. **88**, 079601 (2002).

[30] W. Brandt and M. Kitagawa, Phys. Rev. B **25**, 5631 (1982).

[31] J. D'Avanzo, I. Hofmann, and M. Lontano, Phys. Plasmas **3**, 3885 (1996).

[32] J. D'Avanzo, M. Lontano, E. Tome, and P. F. Bortignon, Phys. Rev. E **52**, 919 (1995).